

# Detecting planet with microlensing

## OUTLINE:

Principle

Example of planet discoveries

Microlensing surveys projects

# Gravitational Microlensing principle

Masses act as lenses by bending light

## **Strong lensing:**

Images of background distant galaxies strongly distorted by foreground mass (massive galaxy or galaxy cluster)

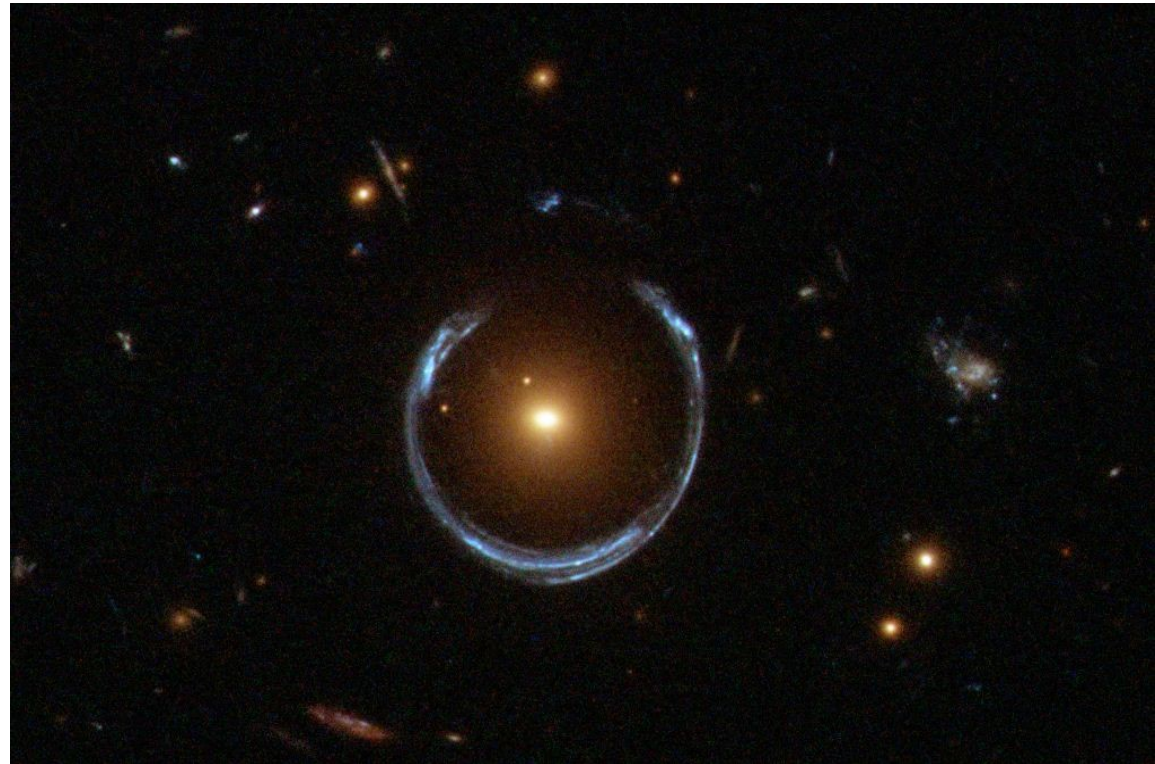
## **Weak lensing:**

Images of background galaxies weakly distorted (slight stretch) by foreground mass. This technique is used to measure and map the mass of galaxy clusters.

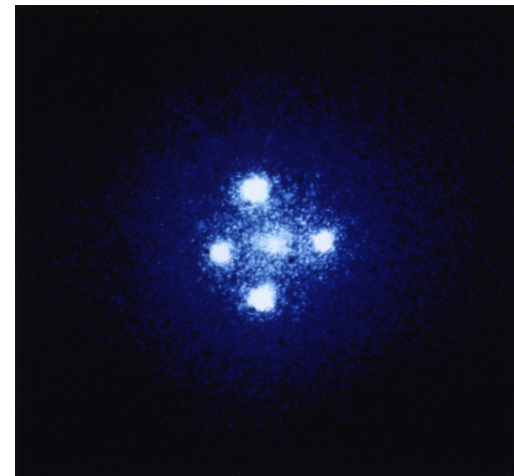
## **Microlensing:**

Flux of star is modulated by foreground star/planet passing along the line of sight.

Technique is used to identify planets



*Examples of strong lensing*



# Microlensing geometry (lens = mass point, source = point source)

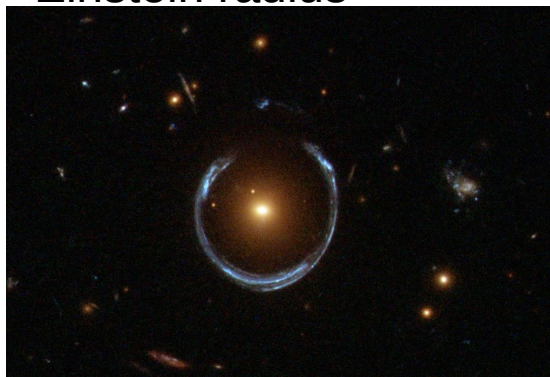
Grav. lens creates two images of the source

- If impact parameter is large: one image is very close to lens and very faint, the other image is almost co-located with true source position
- General case: 2 images, one outside Einstein radius, one inside
- If impact parameter is = 0: the two images become a ring of radius = Einstein radius

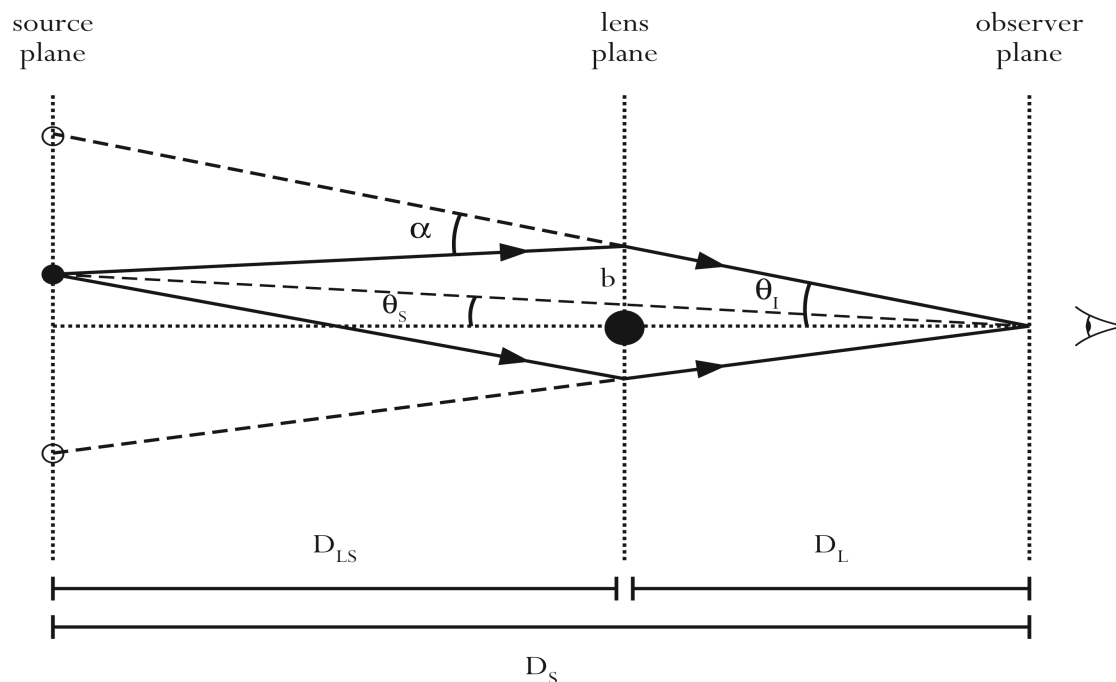
$$R_E = 2 \sqrt{\frac{GMD}{c^2}} = 4.03 \text{ AU} \sqrt{\left(\frac{M}{M_\odot}\right) \left(\frac{D}{2 \text{ kpc}}\right)}$$

reduced distance  
 $1/D = 1/D_L + 1/D_{LS}$

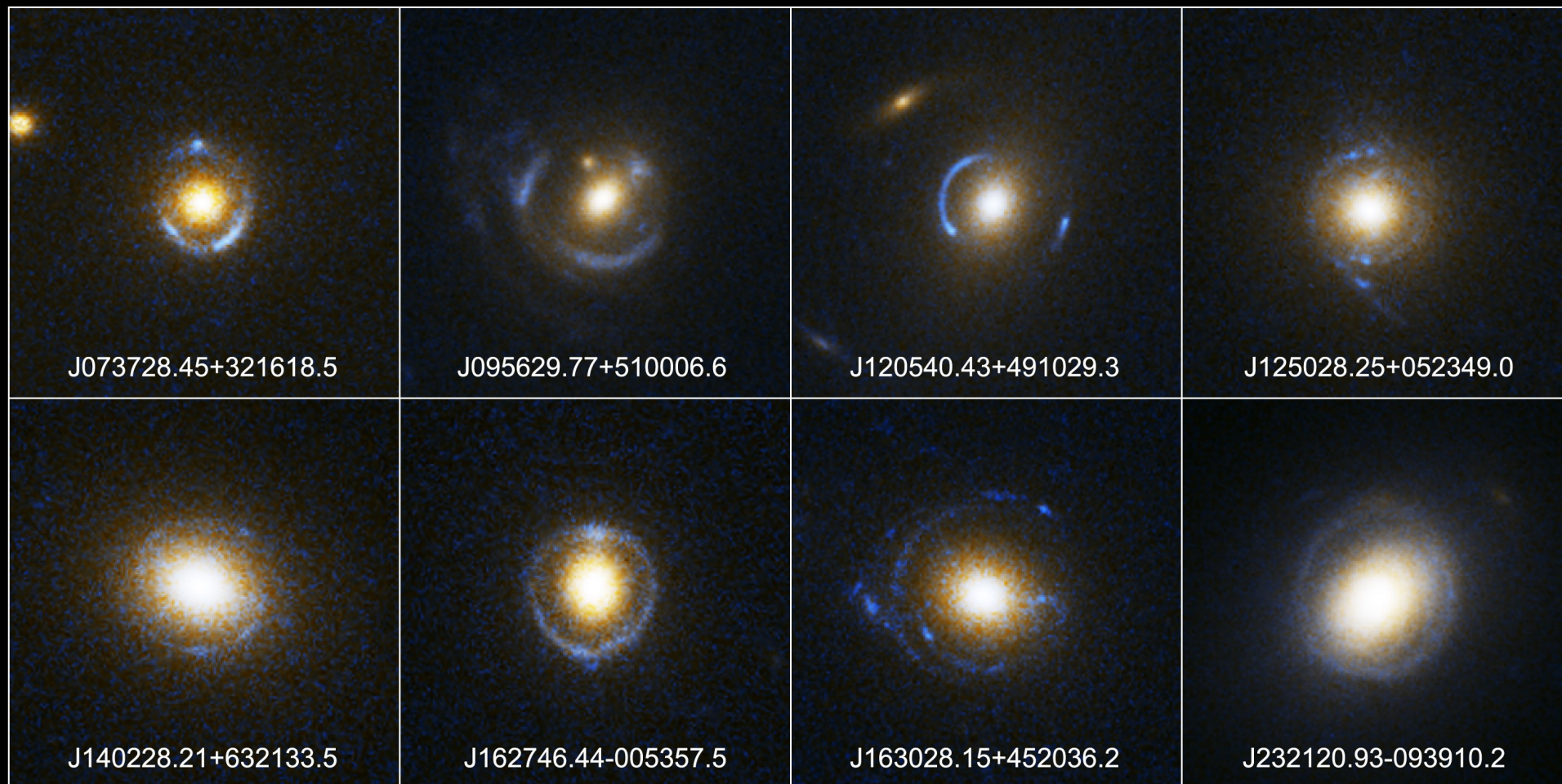
Einstein radius



Lens mass / Solar mass







## Einstein Ring Gravitational Lenses

*Hubble Space Telescope • Advanced Camera for Surveys*

# Microlensing geometry

Einstein radius is usually too small to be resolved  
Planet detection with microlensing relies on photometry

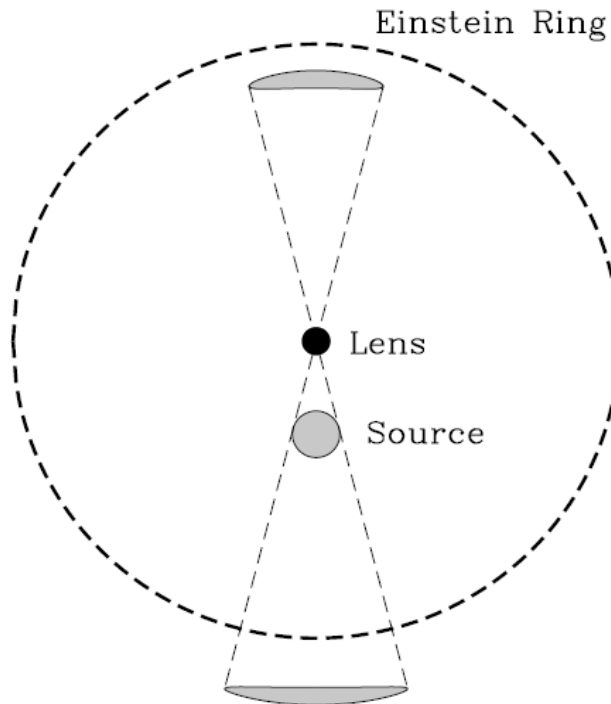


**Fig. 6.** Elongation of the two background source images for the microlensing event model (case 1) discussed in Sect. 3.3, and also shown in Fig. 4. The unlensed source diameter is  $500 \mu\text{arcsec}$ . The image elongation is shown at the moment of the smallest lens-source separation, and the largest magnification during the event.

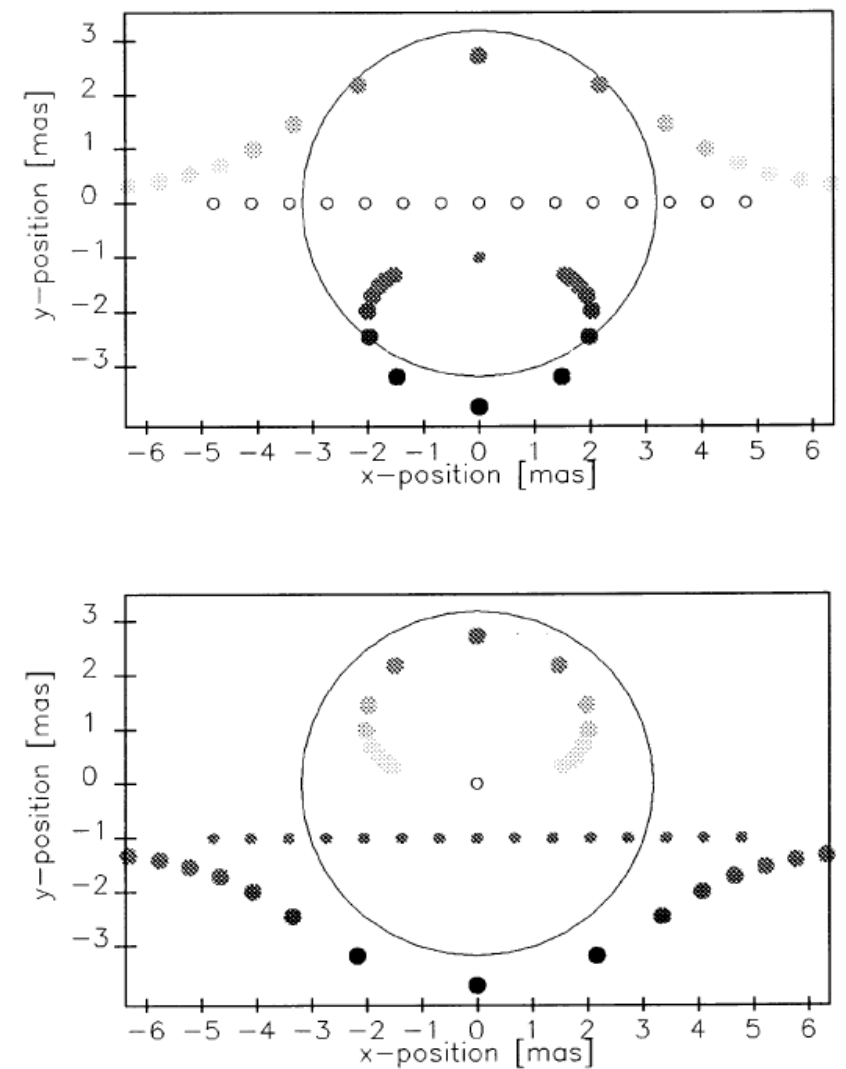


**Fig. 1.** Two representations of a microlensing event with  $D_{\text{source}} = 8 \text{ kpc}$ ,  $M_{\text{lens}} = 10 M_{\odot}$ ,  $D_{\text{lens}} = 4 \text{ kpc}$ , and impact parameter of 1 mas. The radius of the Einstein ring for this event is  $r_E = 3.2 \text{ mas}$ . Top panel — The background source position is fixed on the sky (small grey dot at  $(x, y) = (0, -1) \text{ mas}$ ), and the lens is moving along the  $x$  axis. Instantaneous pairs of lensed images are connected by the lines passing through the consecutive lens positions. Bottom panel — The lens position is fixed at the center of the frame, and the source position is shown moving along the line  $y = -1 \text{ mas}$ .

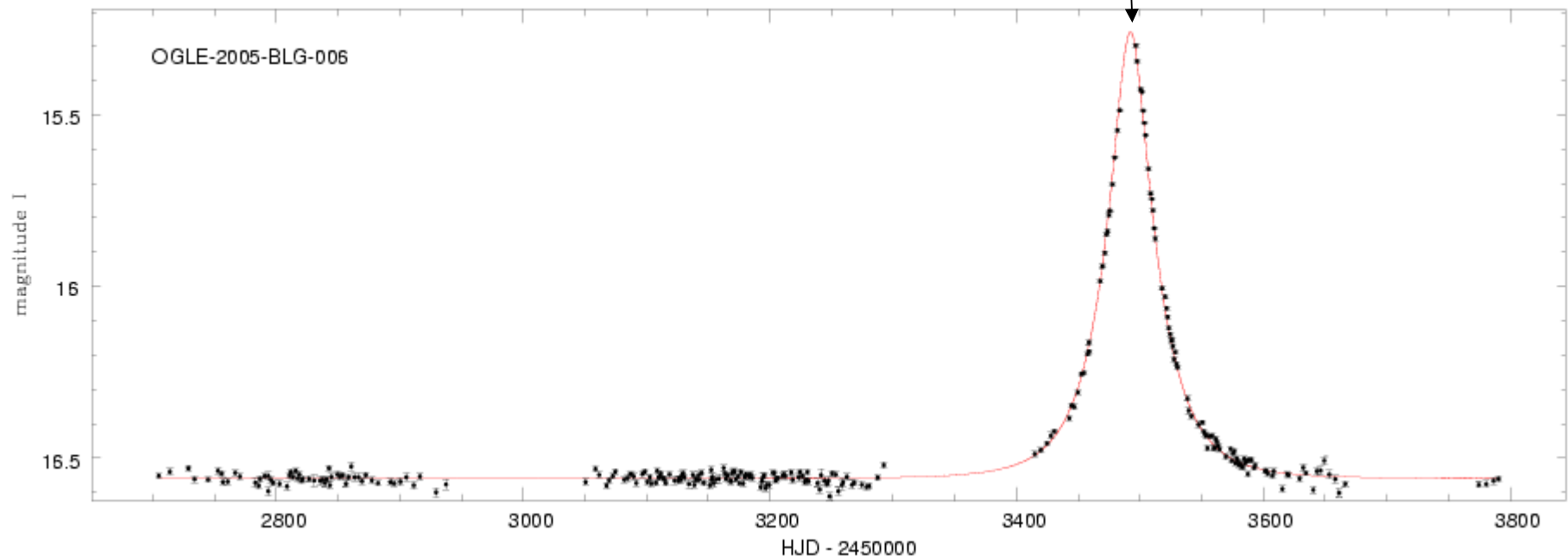
# Microlensing geometry : Flux amplification

$$A = \frac{u^2 + 2}{u\sqrt{u^2 + 4}}; \quad u = \sqrt{u_{\min}^2 + [2(t - t_0)/\hat{t}]^2}$$

Einstein radius crossing time

separation of the lens from source-  
observer line in unit of Einstein

time of max amplification



# Microlensing geometry : Flux amplification with planet

planet has its own  
microlensing  
event

Event is short  
due to smaller  
planet mass

Einstein radius  
is small  $\rightarrow$   
source angular  
size can affect  
lightcurve

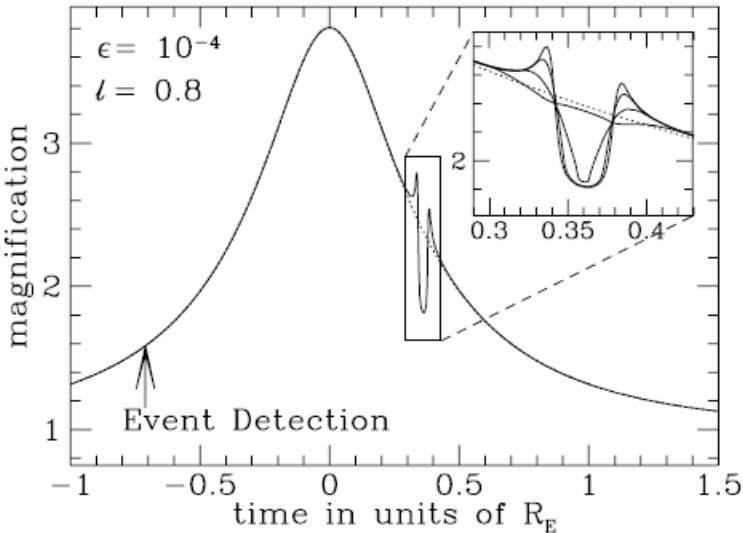


FIG. 1a

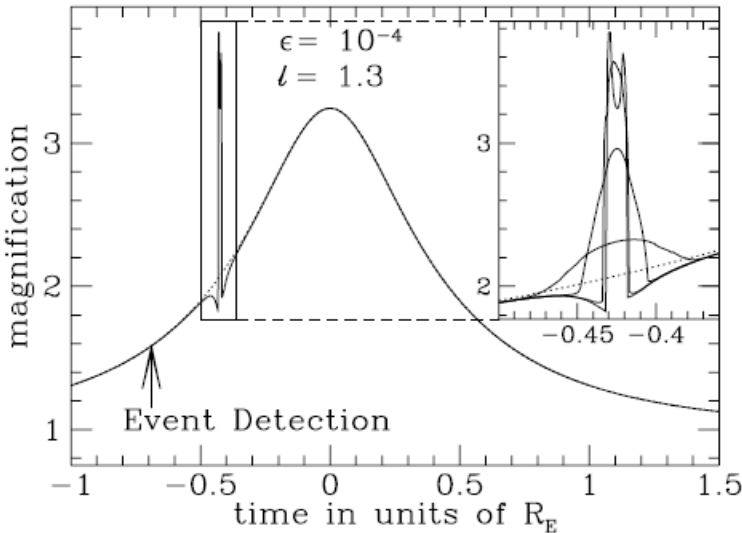


FIG. 1b

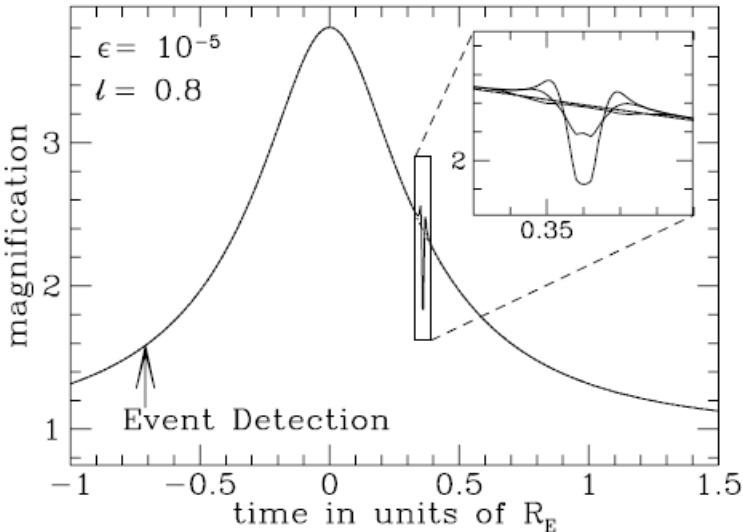


FIG. 1c

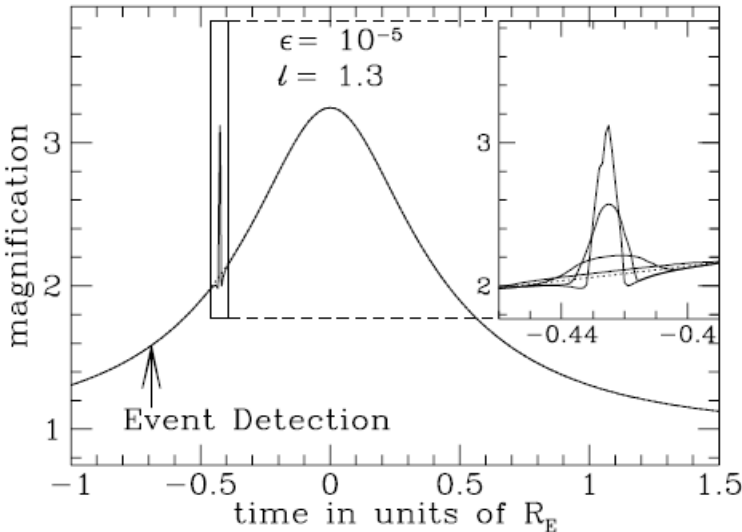


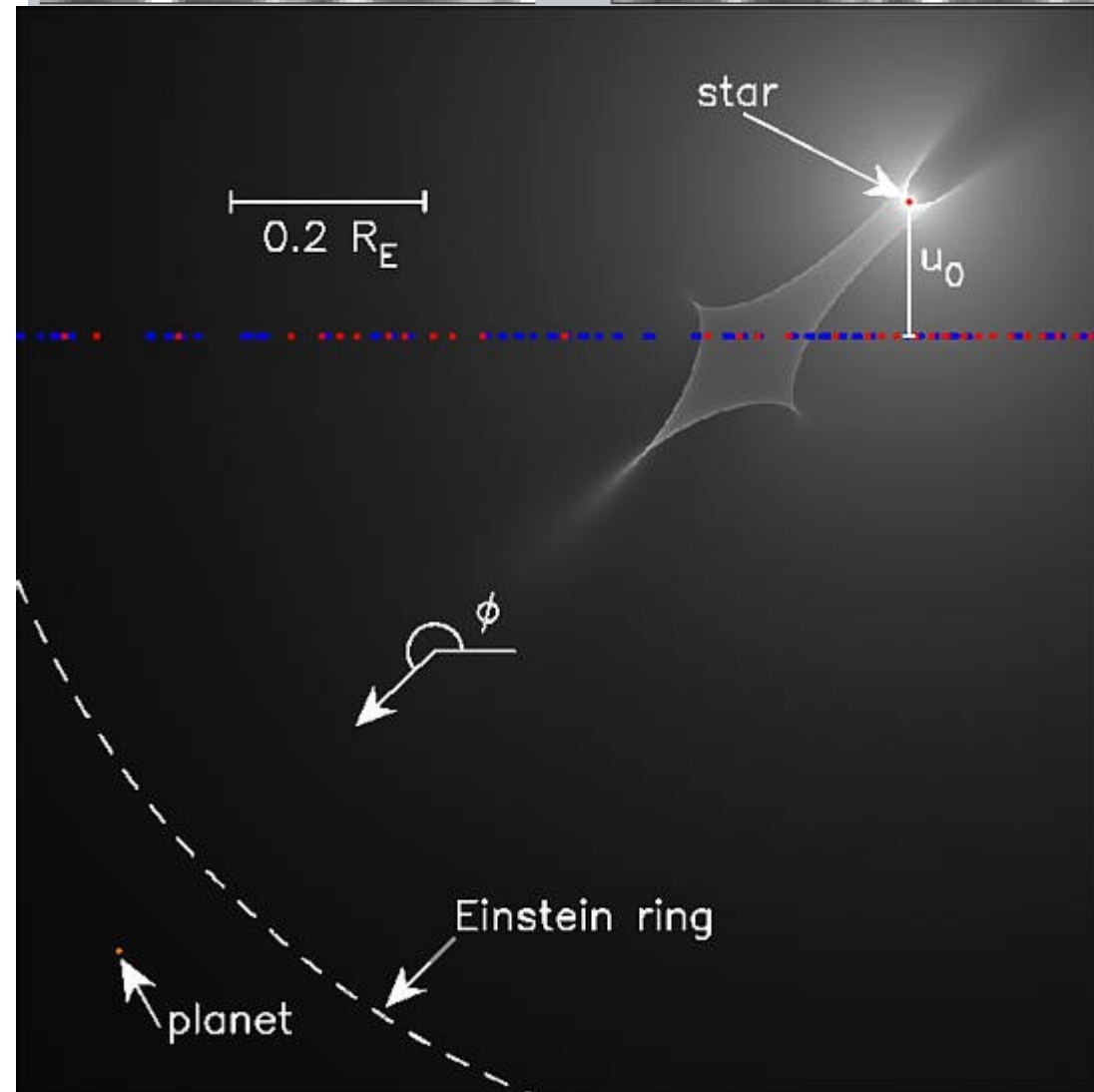
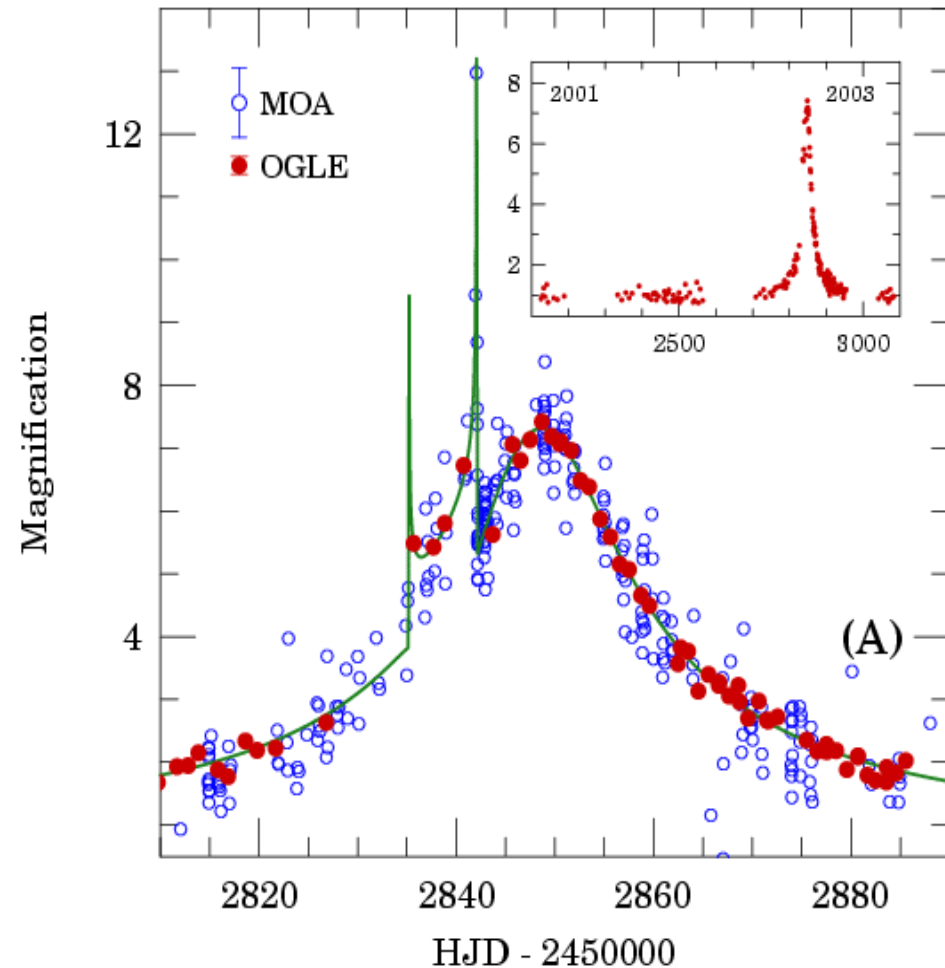
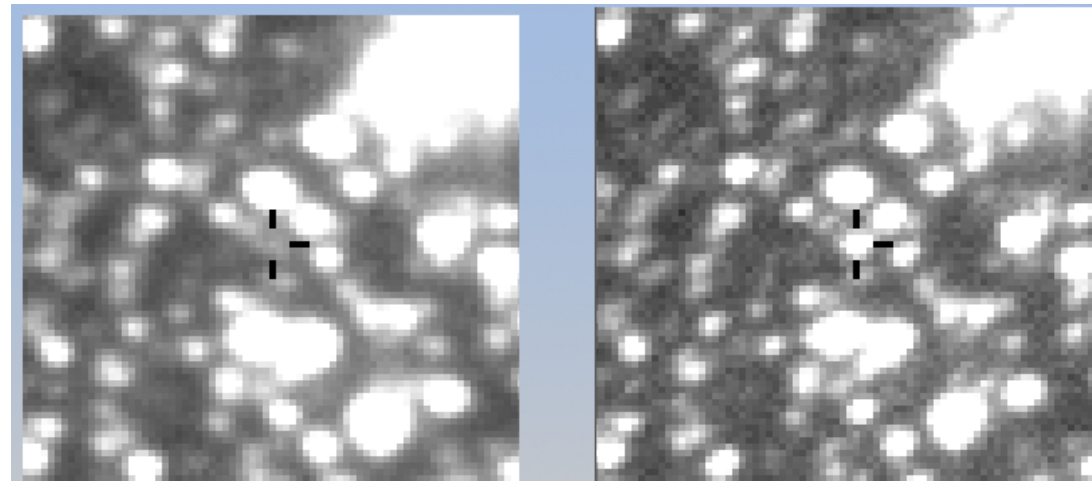
FIG. 1d

FIG. 1.—Microlensing light curves that show planetary deviations are plotted for mass ratios of  $\epsilon = 10^{-4}$  and  $10^{-5}$  and separations of  $l = 0.8$  and  $1.3$ . The main plots are for a stellar radius of  $r_s = 0.003$  while the insets show light curves for radii of  $0.006$ ,  $0.013$ , and  $0.03$  as well. (The amplitude of the maximum light curve deviation decreases with increasing  $r_s$ .) The dashed curves are the unperturbed single lens light curves,  $A_0(t)$ . For each of these light curves, the source trajectory is at an angle of  $\sin^{-1} 0.6 = 36.9^\circ$  with respect to the star-planet axis. The impact parameter  $u_{\min} = 0.27$  for the  $l = 0.8$  plots and  $u_{\min} = 0.32$  for the  $l = 1.3$  plots.



# Microlensing geometry : Flux amplification with planet

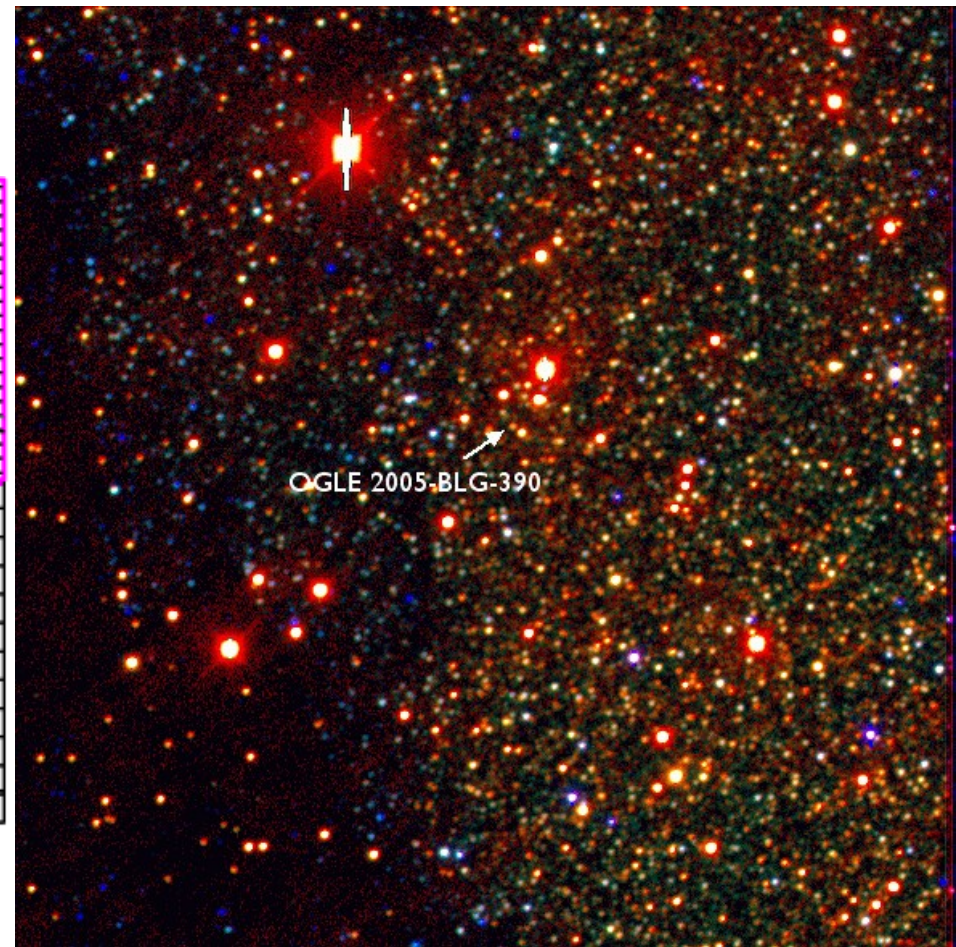
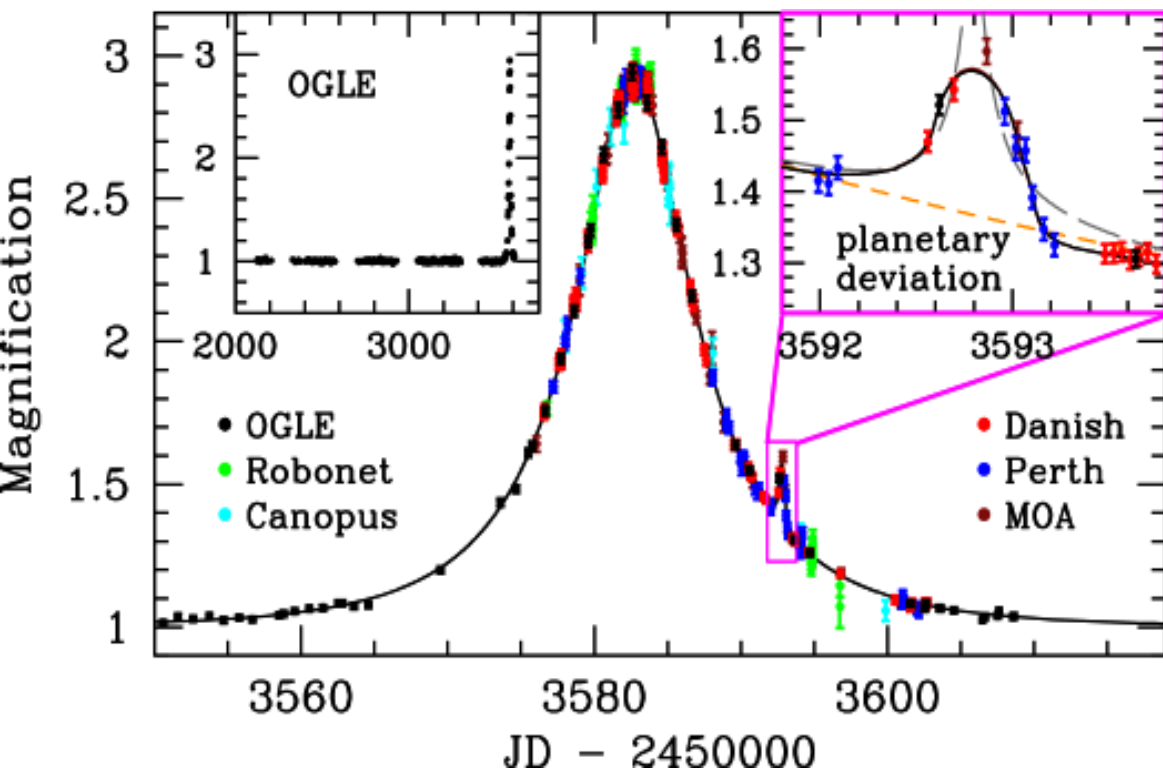
First  
microlensing  
detection of  
massive planet  
(OGLE+MOA)





# Discovery of a 5.5 Earth mass planet

Search strategy: first, identify microlensing event (slow rise in flux seen by OGLE)  
Then, follow-up photometry with multiple telescopes.



# Discovery of a 2-planet system (Gaudi et al. 2008)

Complicated light curve, with large flux amplification as background source moves across caustics.  
→ allows detailed derivation of system geometry, including orbital motion seen during event

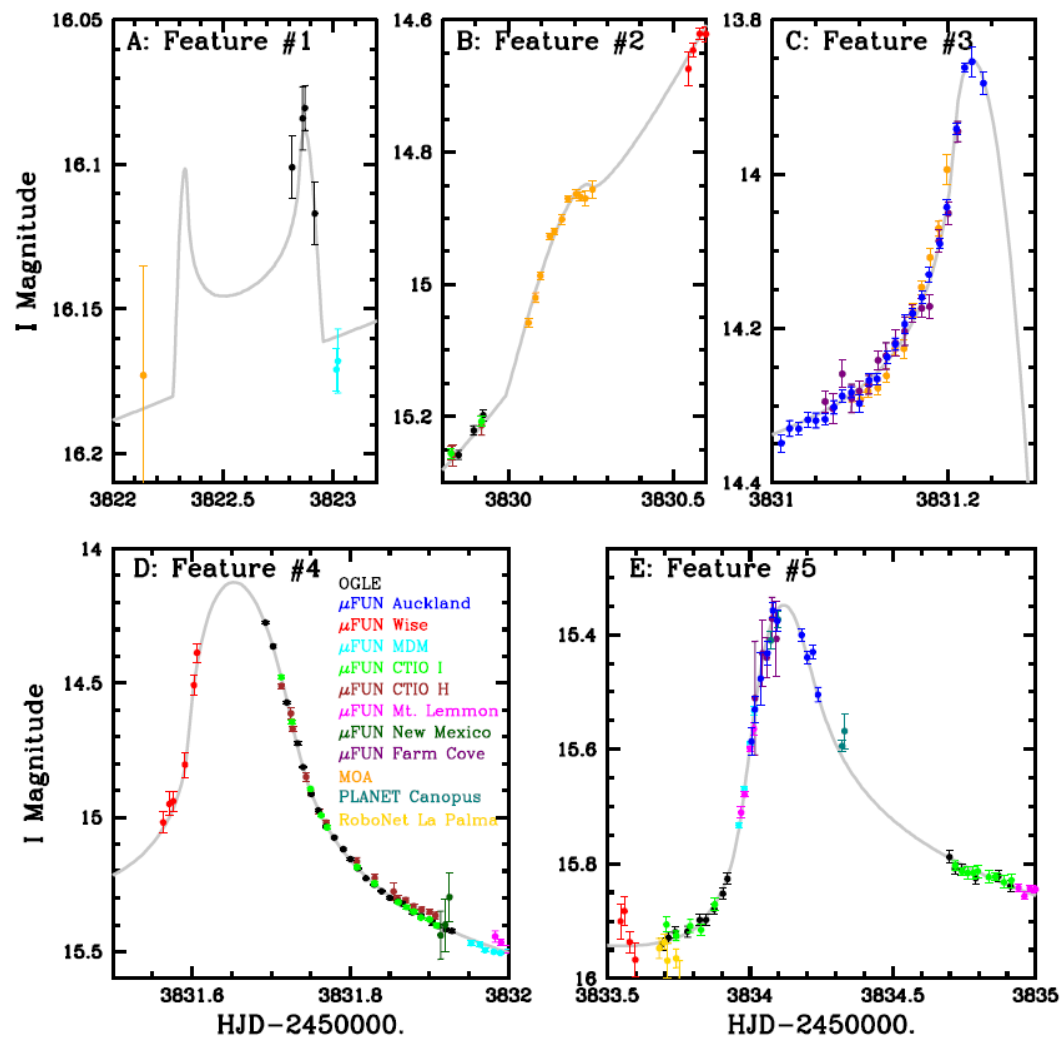
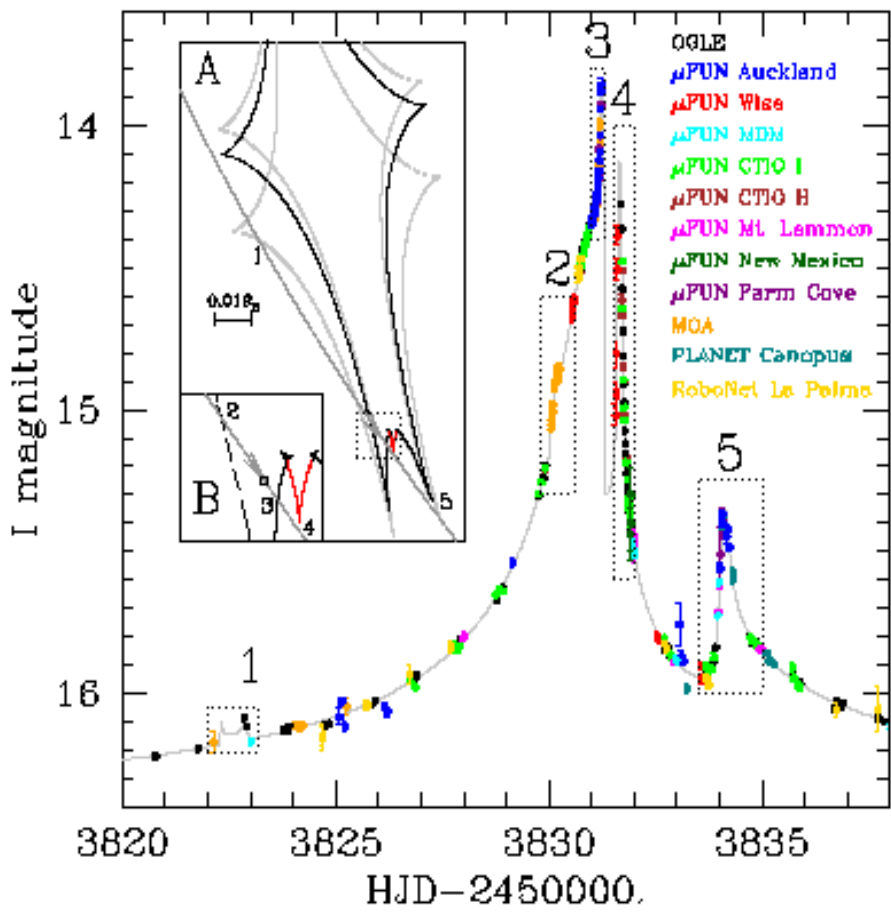


Figure 2: Five features of light curve from Fig. 1 which determine planetary geometry. A) Feature 1: weak cusp crossing; B) Feature 2: weak caustic entrance; C) Feature 3: strong caustic exit; D) Feature 4: strong cusp approach; E) Feature 5: moderate cusp approach. Features 1, 2, 3, and 5, are explained by the black portion of the caustic seen in in Fig. 1A. Feature 4 requires an additional cusp in the caustic, which is shown as the red curve. Data have been binned for clarity.

# Microlensing surveys: goals and challenges

**Low probability event:** need to monitor large number of stars

- probability is smaller than transit
- signal is usually much stronger (amplification  $\sim 2x$ ), easily detectable

**No follow-up possible after event:** planet is only detectable during microlensing event, and host star often cannot be seen

Note: Ground-based imaging after event can identify host star as its image drifts away from background source

Microlensing is **sensitive to outer and isolated planets** that cannot be detected by other techniques → provides valuable complementary information on statistical occurrence of exoplanets, even with small number of detections  
(transit, RV and astrometry are biased to detect planets at small separation)

→ microlensing data suggests that free-floating planets are common  
(Nature 473, 349 (2011))



# The Optical Gravitational Lensing Experiment (OGLE)

## 1.3 m Warsaw University Telescope Las Campanas Observatory, Chile

### Telescope technical data:

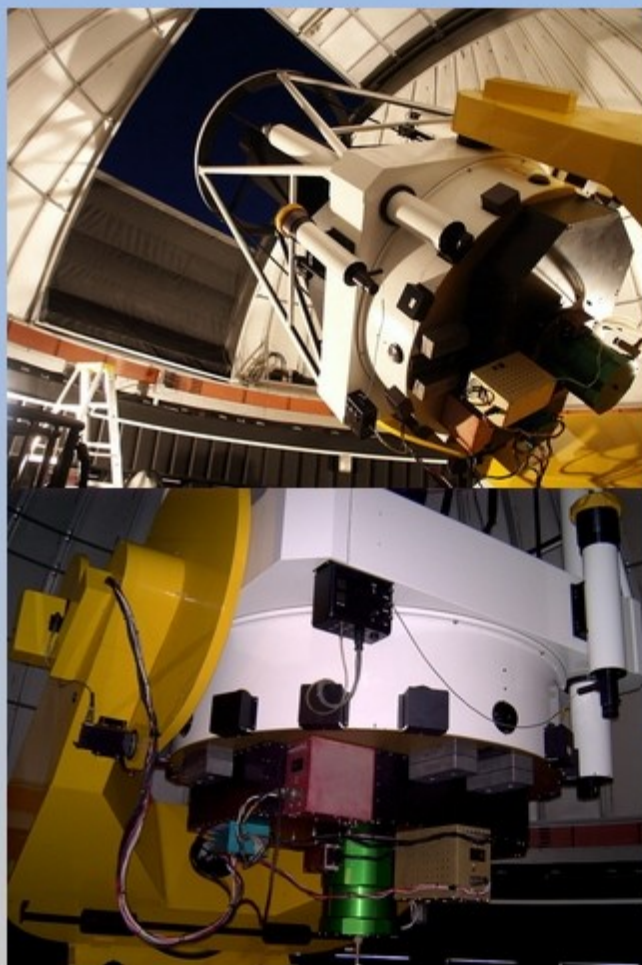
- 1.3m (51") primary mirror diameter
- 1:9.2 (1:2.8 primary) Ritchey-Chretien system; 17.4 arcsec/mm focal scale
- 3-element field corrector - 1.5° diffraction limited field (80% of light within 0.5 arcsec diameter)
- Ultra Low Expansion (ULE) glass mirrors
- Fully automated, computer controlled operation
- Fork, paralactic mount, friction drives (no backlash) allowing any tracking rate in RA and DEC
- Light, steel enclosure with Ash-dome dome, easy ventilation (louvers on telescope and ground level). Minimalization of heat sources in the telescope building
- Remote control of the telescope and instruments from "control building" located 15 m away from the telescope building. Possibility of remote control over the Internet
- First "optical" light Feb 9, 1996, first "electronic" light Jul 18, 1996



Control building (left) and the dome



# The Optical Gravitational Lensing Experiment (OGLE)



The telescope and its instruments

## CCD Camera

- **Single chip camera (OGLE-II, 1997-2001)**
  - SITe 2048×2049 thin chip
  - 90% QE over wide range from *B* to *I*, also some sensitivity in *U*
  - 0.4 arcsec/pixel scale
  - 5 e<sup>-</sup> readout noise at 3.8 e<sup>-</sup>/ADU (16-bit ADC: 65535 levels)
  - modular control system developed at Warsaw University Observatory - easily expandable to multi-chip mosaic, next generation cameras
- **"Second generation" mosaic camera (OGLE-III, 2001-2009)**
  - eight thin SITe 2048×4096 CCD chips (total of 8192×8192 pixels)
  - 0.26 arcsec/pixel scale, 35'×35' total field of view
  - 6-9 e<sup>-</sup> readout noise (depending on chip) at 1.3 e<sup>-</sup>/ADU gain
  - 98 seconds readout time
- **"Third generation" mosaic camera (OGLE-IV, 2009-...)**
  - 32 thin E2V44-82 2048×4096 CCD chips
  - 0.26 arcsec/pixel scale, 1.4 square degrees total field of view
  - 4.5-6.5 e<sup>-</sup> readout noise (depending on chip) at 1.0 e<sup>-</sup>/ADU gain
  - 20 seconds readout time

## Auto-Guiding System and Filter Wheel (OGLE-II and OGLE-III)

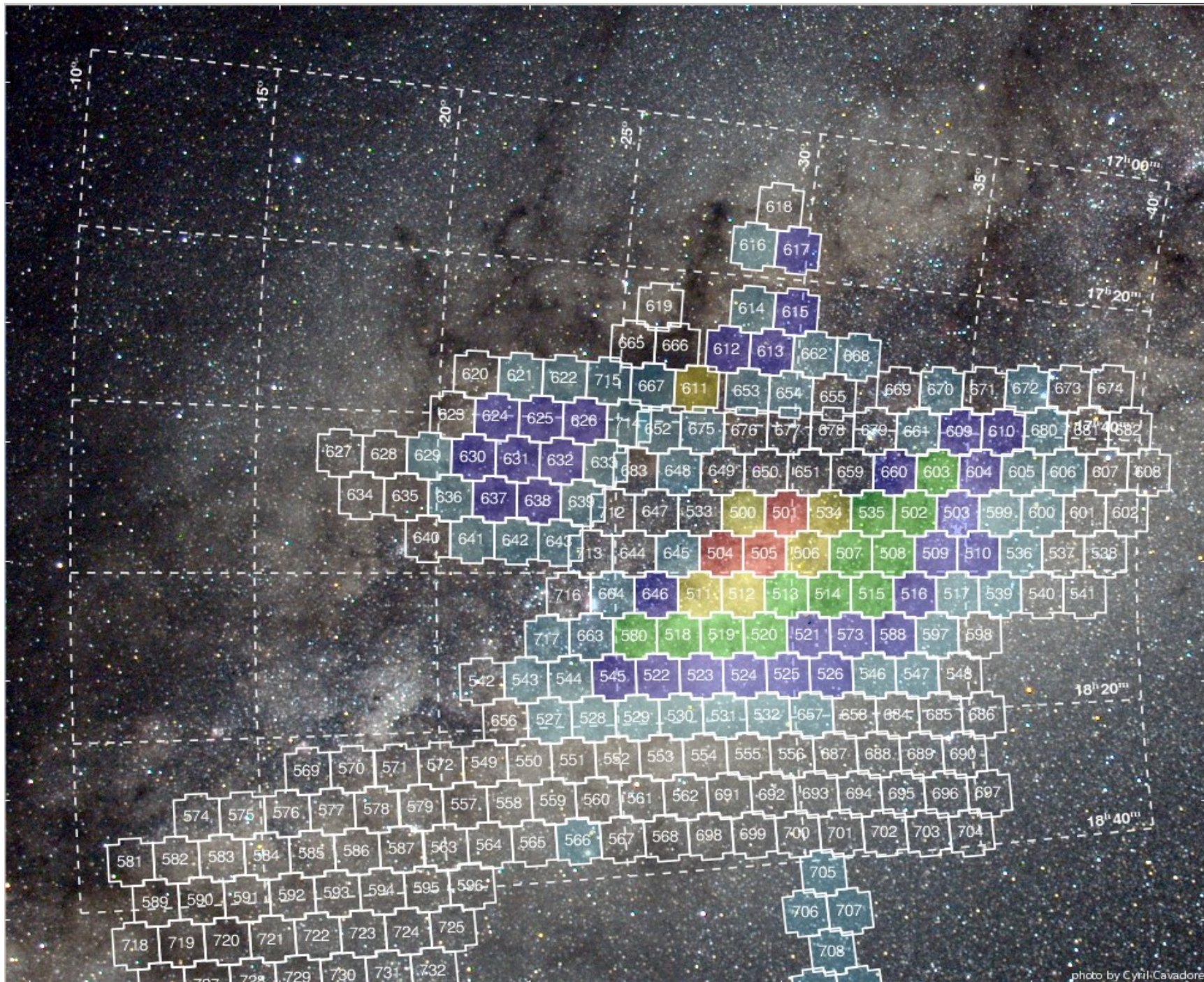
- 512×512 pixels EEV CCD37 detector driven by the same electronics as scientific CCD (2.2" by 2.2 arcmin field)
- Automatic positioning of the guider probe with accuracy of 2 pixels over the entire field of view
- Automatically positioned filter wheel with 7 slots for up to 16 cm diameter filters. Standard *UBVRI* filters installed

## Auto-Guiding System and Filter Holder (OGLE-IV)

- Automatically positioned filter holder with two slots for 31 cm × 31 cm size filters. Standard *VI* interferometric filters installed



# OGLE galactic bulge field (OGLE also includes other fields)



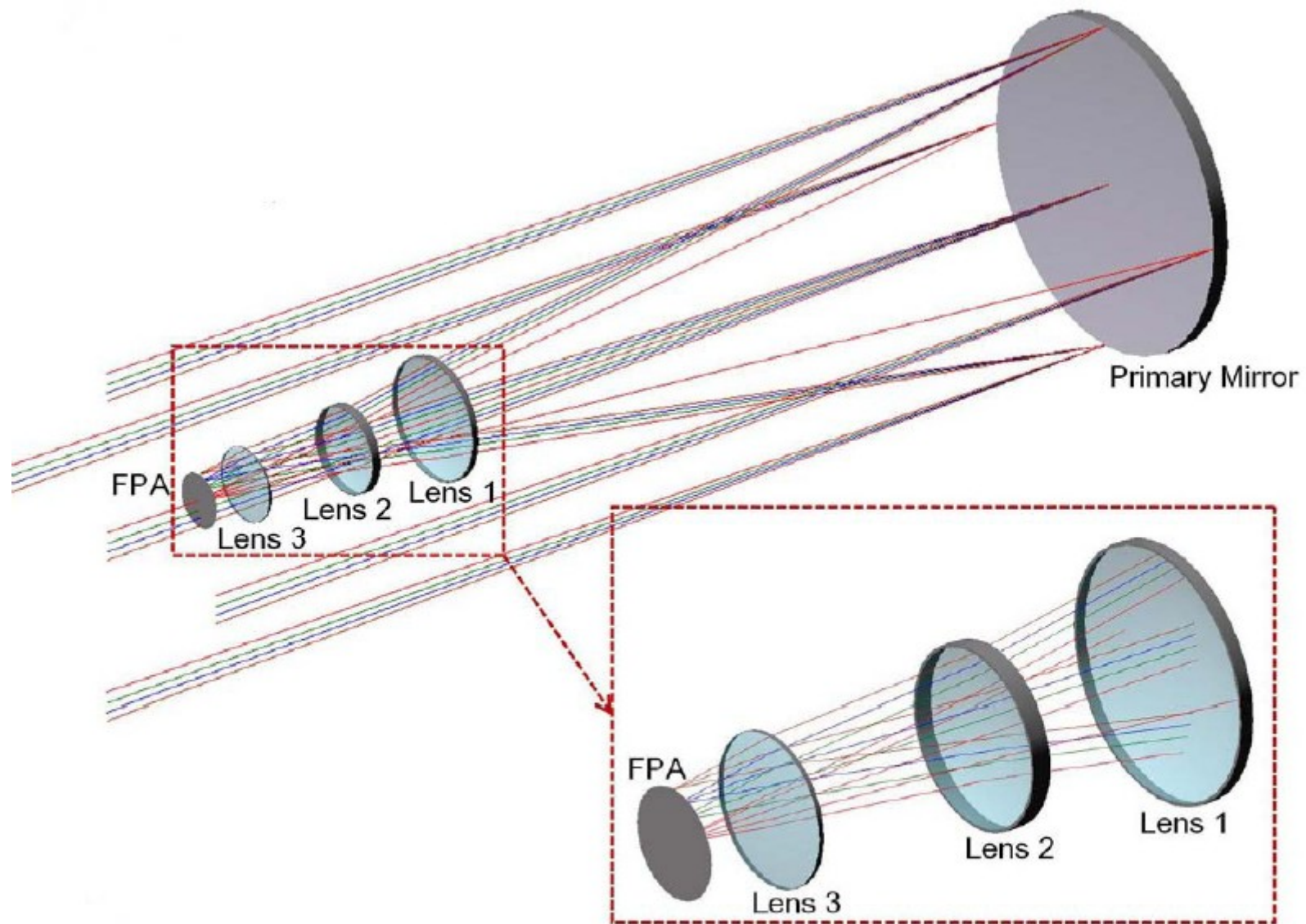


# MOA telescope

1.8-m telescope in New Zealand



# KMTnet (Korean project, 3 wide field telescope, 1.6-m diam each)



One of the optical design with 1.6m,  $f/3.25$ , prime focus and  $4 \text{ deg}^2$  field of view



# Space mission concepts for microlensing

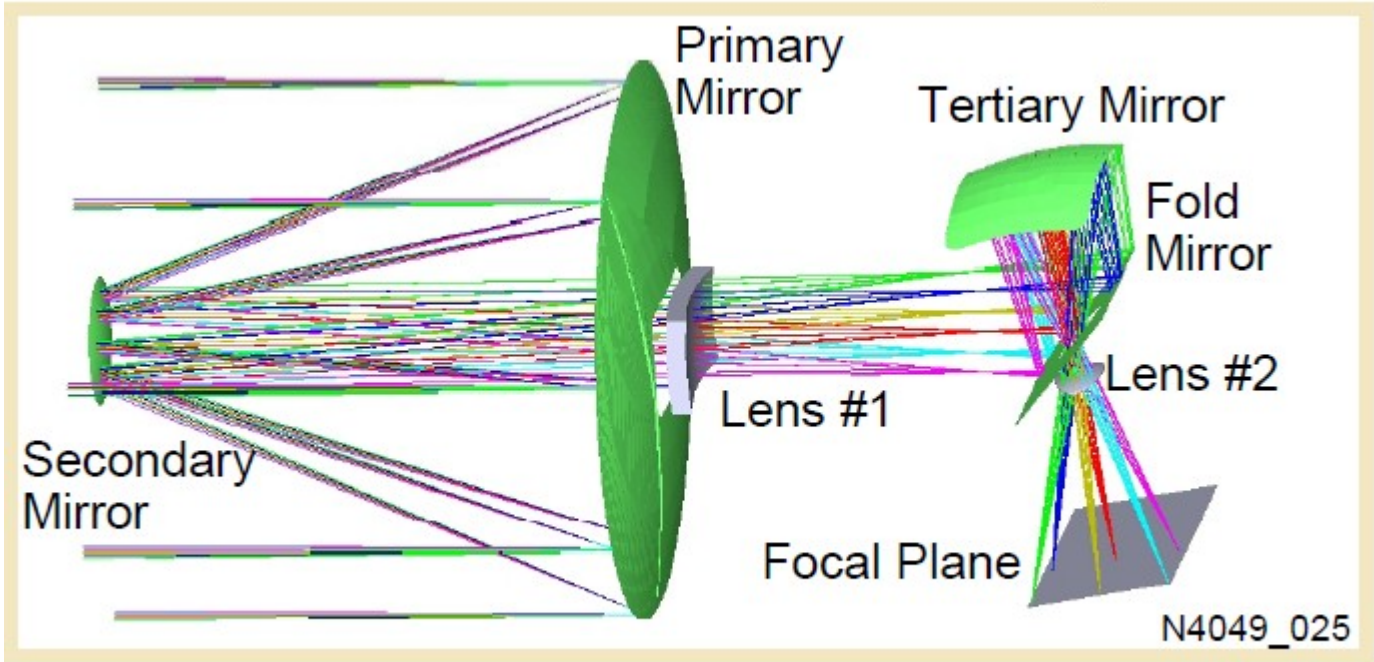
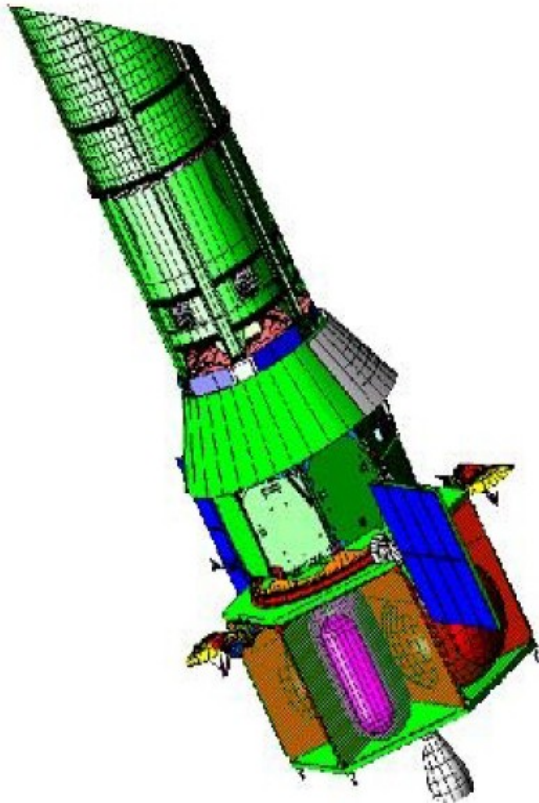
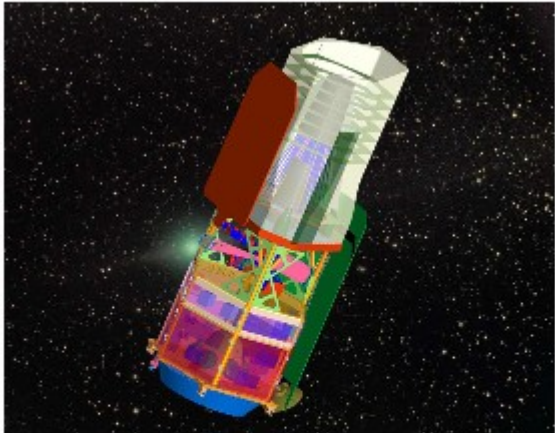


**Fig. 14: MPF Telescope Configuration.**

Microlensing Planet Finder (MPF): 1.1-m telescope, 1.25 sq deg FOV (proposed to NASA)



WFIRST observatory. This is the JDEM-Omega design as specified by the NWNH Decadal Survey. It is a baseline design that is being studied and modified by the Science Definition Team (SDT).

Wide field infrared survey telescope (WFIRST) mission, recently identified as a priority for future mission development, would include a microlensing component.